Low Cost Electrochemical PGE Platform for Sensitive Determination of Pb(II) and Cd(II)

ECS Transactions, 110 (1) 255-272 (2023)
10.1149/11001.0255ecst ©The Electrochemical Society

Low Cost Electrochemical PGE Platform for Sensitive Determination of Pb(II) and Cd(II)

M. A. Saucedo, M. Galicia,[z] and K. A. Carrasco

Department of Chemical Biological Sciences, UACJ, Ciudad Juárez, Chihuahua, 32310, MEXICO

[z]E-mail: monica.galicia@uacj.mx

Low-cost electrochemical platform for sensitive Pb(II) and Cd(II) detection in aqueous solution were fabricated using pencil graphite leads. Cyclic voltammetry (CV) and electrochemical impedance spectroscopy (EIS) were applied to electrochemical characterization of the Pencil Graphite Electrode (PGE). Average electroactive surface was determined as 2.58 times its geometrical area. Parameters for the electrochemical detection of lead and cadmium ions were optimized using Anodic Stripping Square Wave Voltammetry (ASSWV) in 0.1 M HCl (E_{dep}= -1 V, t_{dep}= 60 s). Electroanalysis results exhibited linear increment of electrochemical signals with an increase in the concentration of Pb(II) and Cd(II) in two different ranges. Based on the calibration curve, limits of detection (LOD = 3σ m^{-1}) were 0.946 mg L^{-1} and 1.107 mg L^{-1} respectively. This electrochemical platform constitutes an effective and low-cost approach (0.20 USD per unit) that may be useful to industry, academia, or regulatory agencies.

Introduction

Cadmium and lead are non-essential and toxic heavy metals with adverse health effects. As a consequence of non-strict management of electronic or industrial waste, or activities such as mining, ions of these toxic metals are released into the environment dissolved in an aqueous media, causing contamination of soils and groundwater sources (1-3). Prolonged exposure, even to low concentrations, of lead and cadmium ions can cause a decrease in IQ and increase the risk of cancer, since they can bioaccumulate and inhibit the activity of proteins involved in the synthesis of antioxidants (4,5). Lead affects the nervous system, causing lead poisoning, infants being the most likely to suffer the most serious consequences of this disease (5), and cadmium increases the possibility of suffering from cancer, and in general it is toxic to various systems of the body (6). Due to the adverse health effects of these metallic ions, their concentrations in water are regulated by various organizations around the world, to ensure water quality. The United States Environmental Protection Agency, within the National primary drinking water regulations, establishes the maximum permissible limit for lead at 0.015 ppm and for cadmium at 0.005 ppm (7). Official Mexican Standards NOM-127-SSA1-1994, NOM-002-ECOL-1996 and NOM-003-ECOL-1996 establishes the maximum permissible limits of cadmium and lead ions for drinking water at 0.005 and 0.01 ppm, for wastewater discharged into urban sewage systems in 1 and 2 ppm, and finally, for wastewater reused in public services in 0.4 and 1 ppm, respectively (8-10). Quantification of these metals can be performed by Visible and UV spectrophotometry, although this method has the

disadvantage of using organochlorine solvents such as carbon tetrachloride, a known hepatotoxic agent (11). Currently, atomic absorption spectrophotometry is the most widely used technique for the quantification of heavy metal ions, and in Mexico this is the method that must be used for quantification of metal ions for water quality (12). The determination of heavy metal ions by mass spectrometry using inductively coupled plasma (MS-ICP) is an EPA-approved method for the quantification of heavy metal ions and has the advantage of allowing the detection of multiple analytes at the same time. Nevertheless, its disadvantages are its high costs, not being portable and requiring dedicated personnel to manage the instrument (13,14).

Recently, electroanalytical techniques, such as Square Wave Voltammetry (SWV) have proved as excellent electrochemical alternatives with capacity for sensitive and selective detection of inorganic and organic analytes at trace and ultra-trace levels. In addition, characteristics of this techniques are that they require short analysis times, small amount of samples and presenting ease of implementation (15,16). Electrochemical platforms can be miniaturized with the use of electronic microcomponents (17), being ideal for in-field measurements and saving costs in sample transportation (18). The objective of this research was to develop electrodes with low-cost materials such as pencil graphite leads, to characterize them and test their performance in the simultaneous detection of Pb(II) and Cd(II) in aqueous media. This research may be useful to industry, academia, or regulatory agencies seeking to monitor concentrations of these ions.

Experimental Conditions

Instrumentation.

All electrochemical experiments were conducted using a VSP-300 potentiostat/galvanostat (Bio-Logic Science Instruments®) controlled by the software EC-Lab® V.10.32. A three-electrode cell configuration was used with a platinum wire electrode as counter electrode, a saturated calomel electrode (SCE) as reference electrode and the fabricated Pencil Graphite Electrodes (PGE) and glassy carbon electrodes (GCE, Ø = 3 mm) as working electrodes.

Electrode Fabrication.

Five working electrodes were built using commercial HB #2 pencil graphite leads of 0.5 mm in diameter, epoxy resin as insulator and a copper wire as conductor. The graphite leads were sonicated (Chicago Electronic®) in ethanol (99%, J. T. Baker) during 30 min to clean possible impurities from the manufacturing process. Later they were allowed to dry and were sonicated for 30 min in deionized water and left air dry (19). Finally, they were introduced into a rigid plastic mold to support the electrode, and a copper wire was soldered to one end of the lead and the mold was filled with epoxy resin (20). Once the resin had cured, sandpaper was used to expose the cross section of the graphite and was polished using a 0.5 μm alumina suspension and cloth (21). Process of fabrication is depicted in Figure 1.

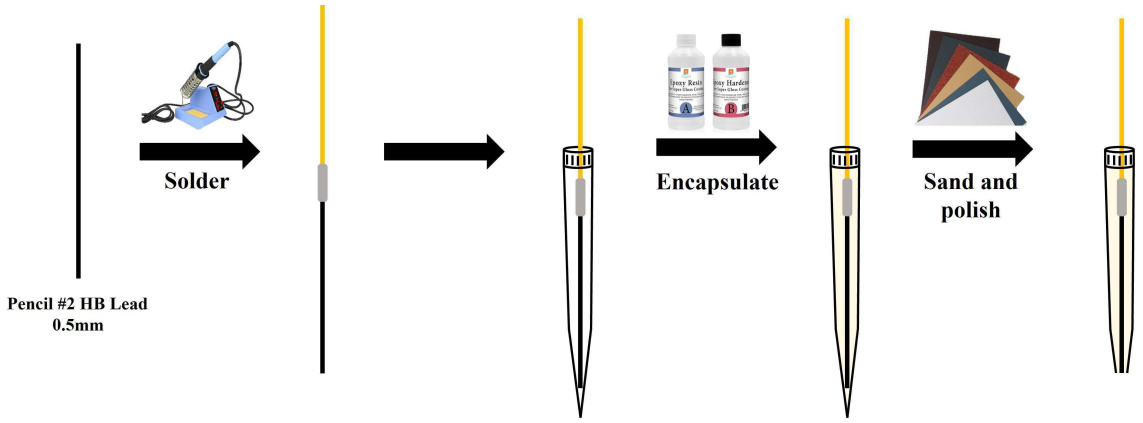

Figure 1. Pencil Graphite Electrode (PGE) fabrication process.

Surface Characterization.

Micrographs of the surface morphology and the elemental composition of the fabricated electrodes were obtained by scanning electron microscopy (SEM) and X-ray energy dispersion spectroscopy (EDS) respectively using a JEOL JSM-7000F scanning electron microscope.

Electrochemical Characterization.

A solution of 5 mM potassium ferrocyanide ($K_4[Fe(CN)_6]$) (99%, Sigma), 5 mM potassium ferricyanide ($K_3[Fe(CN)_6]$) (99%, Sigma) and 0.1 M potassium chloride (99%, J. T. Baker) was prepared as a redox probe to electrochemically characterize the fabricated electrodes (22).

Cyclic Voltammetry. Cyclic voltammograms were obtained using the fabricated PGE as working electrodes in the $[Fe(CN)_6]^{3-/4-}$ solution between -0.2 and 0.6 V *vs* SCE at different scan rates (50, 100, 200, 300, 400, 500, 600, 700, 800 mV s^{-1}) (23). The anodic and cathodic peak currents (I_{pa} and I_{pc}) were determined and plotted *vs* the square root of the scan rate ($v^{1/2}$) and the slope of the curve was used to calculate the electroactive area of the PGE electrodes. The reproducibility of the fabricated electrodes was tested by obtaining the peak current recorded for the system $[Fe(CN)_6]^{3-/4-}$ at a scan rate of 100 mV s^{-1} and applying a one way ANOVA ($\alpha = 0.05$) to the resulting data.

Electrochemical Impedance Spectroscopy. Impedance spectrums were obtained using as working electrode the fabricated PGE and a GCE in the $[Fe(CN)_6]^{3-/4-}$ solution between 10 mHz and 6000 kHz imposing a sinusoidal amplitude of 10 mA (23). Data was simulated using circuit analogs and an equivalent Randles circuit was fitted using the software EC-Lab® V.10.32 (Bio-Logic Science Instruments).

Analytical Electrochemistry.

All electroanalytical determinations were conducted using anodic stripping square wave voltammetry (ASSWV). Solutions of $CdCl_2$ (99%, Merck) and $Pb(NO_3)_2$ (99%, Merck) were prepared at a concentration of 1000 mg L^{-1} Pb(II) and Cd(II) in deionized water.

Supporting Electrolyte Selection. Electrolyte solutions of 0.1 M nitric acid (70%, Sigma), 0.1 M sulfuric acid (98%, Sigma), 0.1 M hydrochloric acid (37%, Sigma), 0.1 M potassium chloride (99%, J. T. Baker) and 0.1 M acetate buffer at pH 4.6 were prepared (24). Using the 1000 mg L^{-1} solutions of Pb(II), Cd(II) and the different electrolytes, 10 mg L^{-1} solutions of the ions were used to select the optimum supporting electrolyte.

Optimization of the Experimental Parameters. A 1 mg L^{-1} solution of Pb(II) and Cd(II) was prepared using 0.1 M HCl as supporting electrolyte. The preconcentration potential, preconcentration time, pulse height (P_H), pulse width (P_W) and step height (S_H) were optimized by plotting the variable to optimize respect to peak current (I_p). The optimal value was selected as the one that provided the highest I_p without distorting the shape of the peaks (24-26).

Analytical Parameters. Solutions of Pb(II) and Cd(II) were prepared at 0.8, 1, 5, 10, 15, 30, 50, 70, 85 and 100 mg L^{-1}, ASSWV were run in triplicate on each in order to generate a calibration curve (concentration *vs* I_p) for both metal ions (19,26). Limits of detection and quantification were calculated using the standard deviation of the linear regression of the calibration curve.

Results

Surface Characterization.

SEM micrographs of the pencil graphite electrode surfaces show their cross-sections revealing that they are composed of graphite flakes (27) (Figure 2A and 2B). The electrode surface is far from flat, it presents a real surface area greater than the geometric one and forms cavities like those that can be observed at 5000x (Figure 2C). In Figure 2D it is possible to observe a rough relief in which white particles can be identified due to their low electronic conductivity.

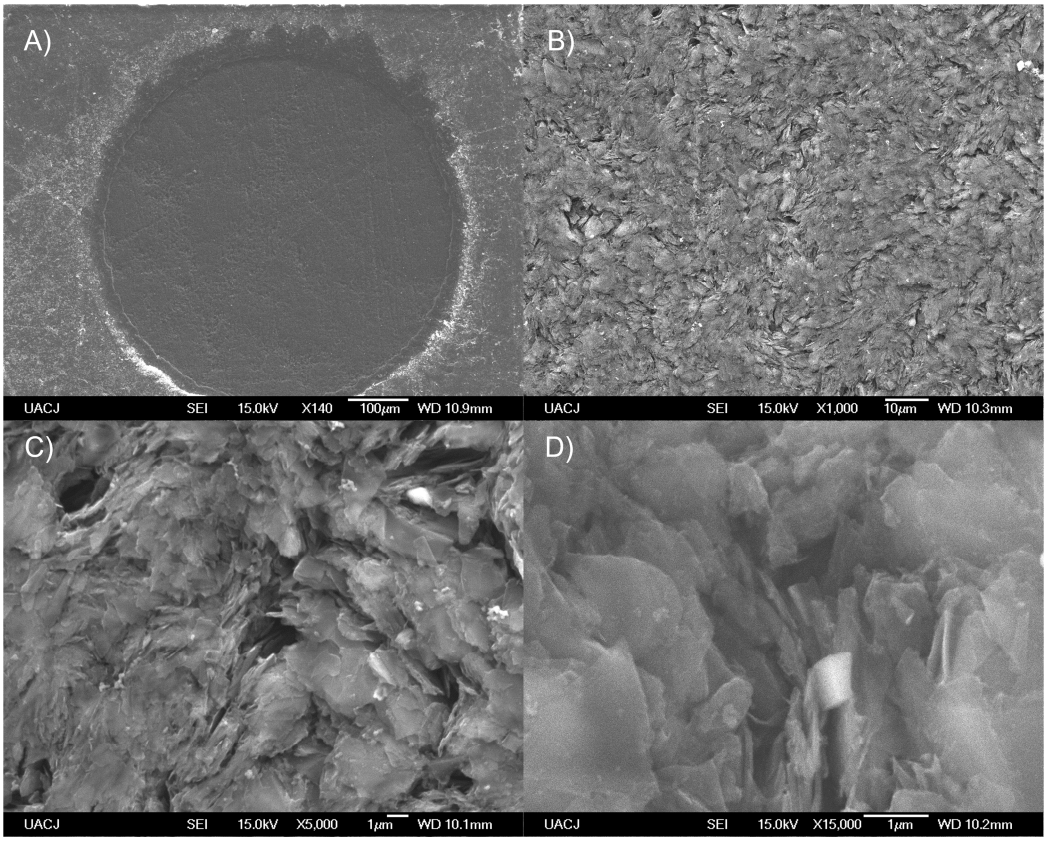

Figure 2. SEM micrographs of the exposed cross section of the Pencil Graphite Electrode (PGE). A) 140X, B) 1000x, C) 5000x and D) 15000x.

The EDS spectrum taken from the electrode surface shows that it is mostly made up of carbon (Figure 3), present due to graphite. In addition, elements such as sodium, aluminum, silicon, chlorine and potassium are found, these are commonly found in clays, such as those used in the manufacturing process of graphite leads (15) (Figure 3).

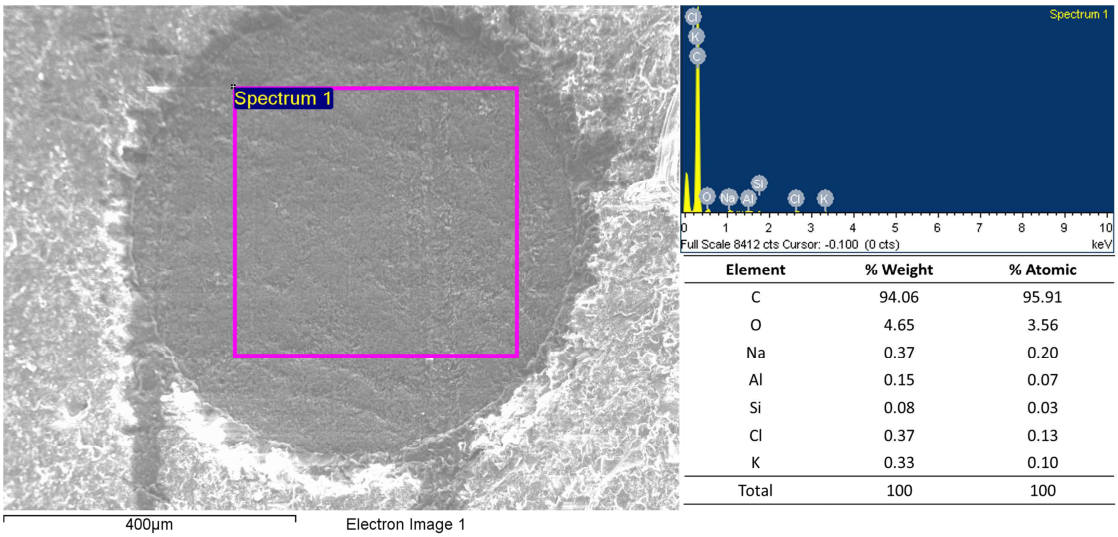

Element	% Weight	% Atomic
C	94.06	95.91
O	4.65	3.56
Na	0.37	0.20
Al	0.15	0.07
Si	0.08	0.03
Cl	0.37	0.13
K	0.33	0.10
Total	100	100

Figure 3. EDS spectrum of the surface of the fabricated Pencil Graphite Electrode (PGE).

Likewise, the elemental composition of the particles of low electronic conductivity found on the surface of the electrode were analyzed and it was found that these are made

up of carbon, oxygen, sodium, magnesium, aluminum, potassium, and calcium (Figure 4), the presence of these elements suggests the use of clays in the manufacturing process of the graphite leads (15).

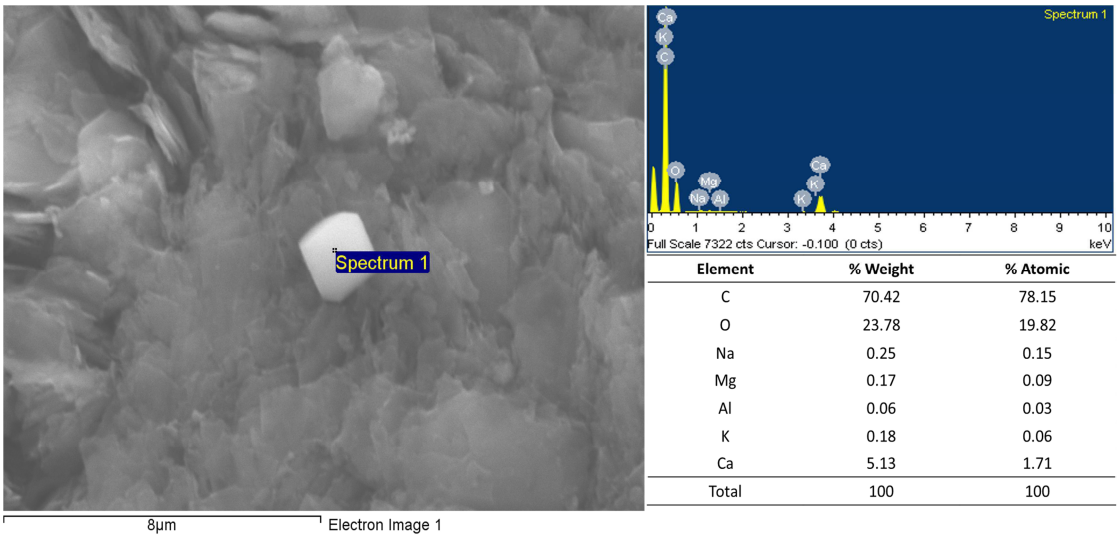

Element	% Weight	% Atomic
C	70.42	78.15
O	23.78	19.82
Na	0.25	0.15
Mg	0.17	0.09
Al	0.06	0.03
K	0.18	0.06
Ca	5.13	1.71
Total	100	100

Figure 4. EDS spectrum of a non-conductive particles found in the electrode surface.

Electrochemical Characterization.

Cyclic Voltammetry. The electrochemical behavior of the electrode was evaluated by CV using the $[Fe(CN)_6]^{3-/4-}$ system as redox probe. In the voltammograms obtained at different scan rates, two peaks are observed, one of oxidation at 221.4 mV and the other of reduction at 151.8 mV (Figure 5), which indicates that charge transfer reactions are carried out on the surface of the electrode. The difference between the anodic and cathodic peak potentials is 69.6 mV, while the ratio of the anodic peak current (I_{pa}) to the cathodic peak current (I_{pc}) is 0.99; both values correspond to values close to the ideals for electrochemically reversible processes, 57 mV and 1.00 respectively (21). The fact that the PGE as working electrode exhibits a behavior close to ideal in the $[Fe(CN)_6]^{3-/4-}$ system suggests that the material it is made of is a good candidate for the development of charge transfer reactions.

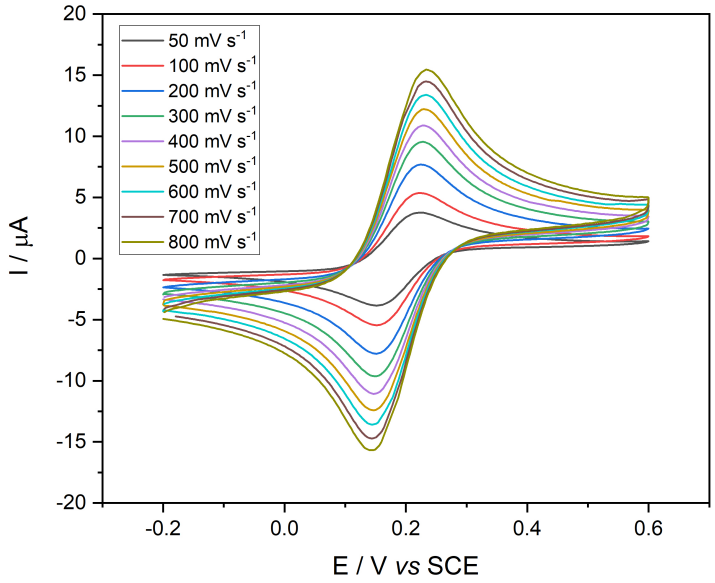

Figure 5. Cyclic voltammograms at different scan rates in 5 mM $[Fe(CN)_6]^{3-/4-}$ in 0.1 M KCl with PGE as working electrode.

The anodic and cathodic peak currents were obtained from the voltammograms at different scan rates (Figure 5) and with them curves of the square root of the scan rate ($v^{1/2}$) with respect to the peak current value (I_p) were constructed. It was found that both processes, oxidation and reduction, fit a linear model (Figure 6), which suggests that both processes are controlled by mass transport, specifically, by diffusion (28).

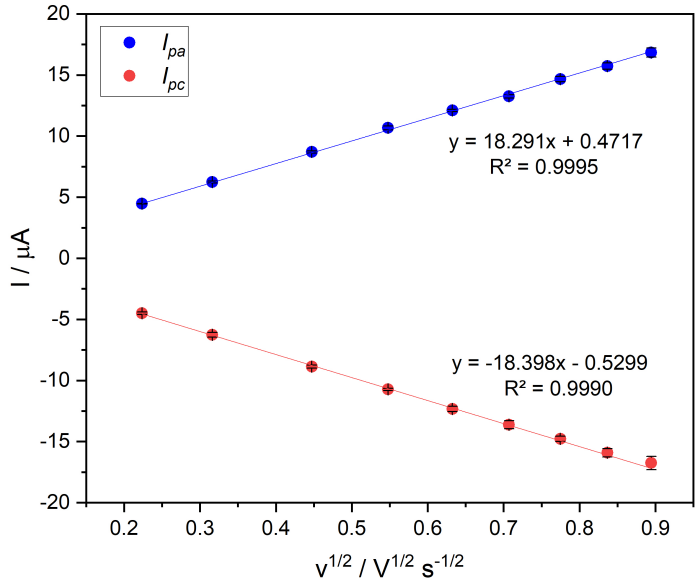

Figure 6. Plot of the square root of the scan rate *vs* peak current in 5 mM $[Fe(CN)_6]^{3-/4-}$ in 0.1 M KCl with PGE as working electrode.

The slope of the anodic current curve (Figure 6) was used to calculate the average electroactive area of three different PGE by means of the Randles-Sevcik equation (Equation 1).

$$I_p = 2.69 \times 10^5 \, n^{3/2} \, A \, D^{1/2} \, C \, v^{1/2} \quad [1]$$

Where I_p is the peak current in amperes, n is the number of electrons transferred in the process (1), D is the diffusion coefficient of the species (7.2 x 10^{-6} cm^2 s^{-1} (29)), C is the concentration in mol cm^{-3} (5 mol cm^{-3}), v is the scan rate in V s^{-1} and A is the electroactive area in cm^2.

It was found that the average electroactive area of the PGE is 5.07 x 10^{-3} ± 1.2 x 10^{-4} cm^2, a value 2.58 times greater than its geometric area, 1.96 x 10^{-3} cm^2, data that is supported by the microstructure of the electrode observed in the SEM micrographs (Figure 2).

The current per unit area, current density (j), obtained using a glassy carbon electrode (GCE) was compared with that obtained using a PGE as working electrode (Figure 7) and it was found that the latter presents a current density 0.82 times that of the GCE.

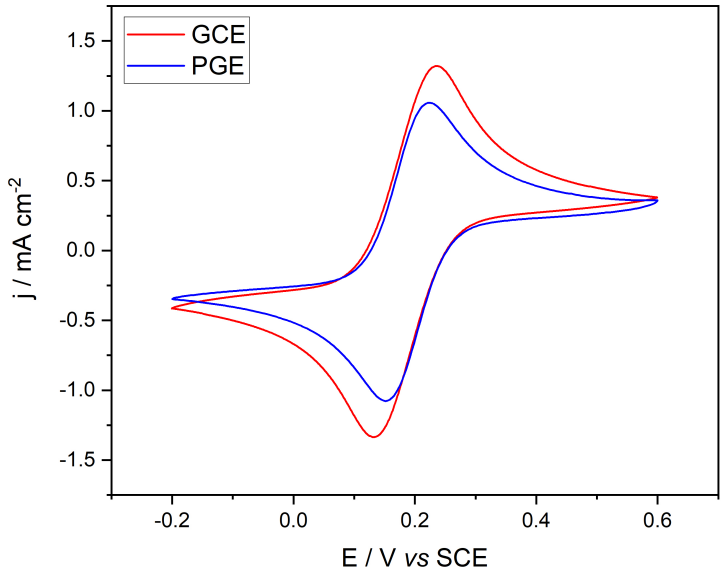

Figure 7. Normalized voltammograms recorded at 100 mV s^{-1} in 5 mM $[Fe(CN)_6]^{3-/4-}$ in 0.1 M KCl with PGE and GCE as working electrodes.

To assure that the fabricated electrodes are reproducible, three different PGE were used to carry out cyclic voltammetry in the system $[Fe(CN)_6]^{3-/4-}$ and the peak currents were statistically analyzed by a one factor ANOVA. The average peak current was 4.72 ± 0.04 µA and the ANOVA results show that the peak currents obtained with fabricated electrodes are statistically equal ($p < 0.05$) (Figure 8).

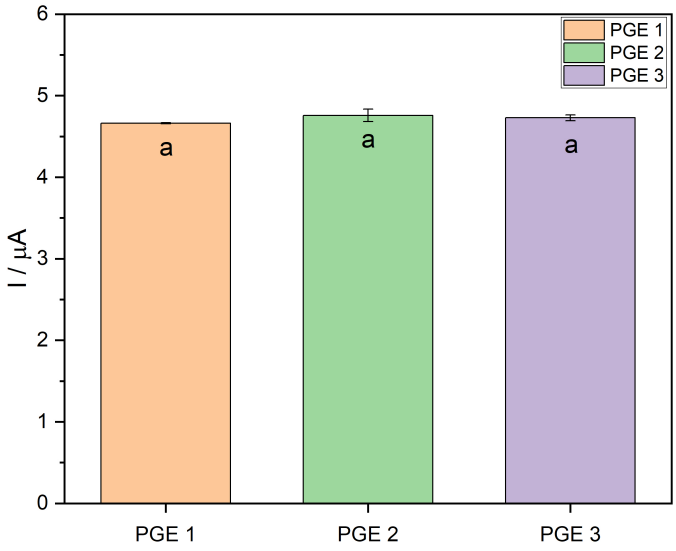

Figure 8. Peak currents recorded at 100 mV s^{-1} in 5 mM $[Fe(CN)_6]^{3-/4-}$ in 0.1 M KCl with three different PGE working electrodes. Equal letters indicate statistical equality ($p < 0.05$).

Electrochemical Impedance Spectrum. EIS were obtained for the PGE and the GCE (Figure 9) to calculate the resistance to charge transfer (R_{ct}) for both electrodes. The Nyquist diagrams show a semicircular region associated with a charge transfer process and a region at approximately 45° to the X axis associated with a diffusional process (30).

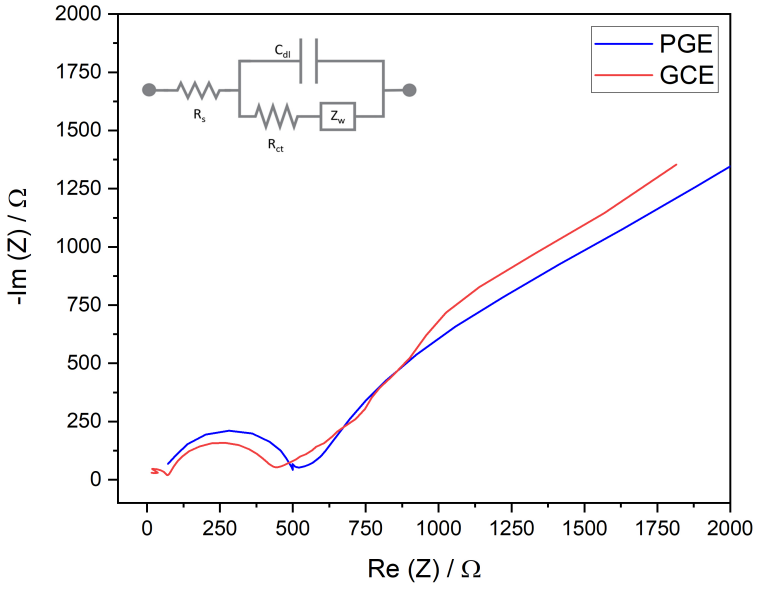

Figure 9. Nyquist plot obtained in 5 mM $[Fe(CN)_6]^{3-/4-}$ in 0.1 M KCl with PGE and GCE as working electrodes and the equivalent Randles Circuit used for EIS fitting.

The Randles equivalent circuit present in Figure 9 was adjusted to the impedance spectra obtained for both electrodes, through which the values of the solution resistance (R_s), double layer capacitance (C_{dl}), resistance to charge transfer (R_{ct}) and Warburg impedance (Z_w) were obtained (Table I). The PGE presents a R_{ct} value of 417.4 Ω, similar to previously reported values (31), also 1.18 times greater than that of the GCE, however, in the same order of magnitude, and a capacitance three orders of magnitude smaller. The results indicate that it is slightly more complicated to carry out charge transfer reactions using PGE as a working electrode due to its higher R_{ct} and that it accumulates less charge on its surface, since it has a remarkably lower capacitance than that of the GCE (30).

TABLE I. Double layer electrical parameters obtained for the electrochemical impedance spectra of PGE and GCE.

Electrode	R_s (Ω)	C_{dl} (μF)	R_{ct} (Ω)	Z_w (kΩ $s^{-1/2}$)
GCE	80.01	0.2244	353.5	357.6
PGE	66.29	0.3205×10^{-3}	417.4	15738

R_s: Resistance of the solution. C_{dl}: Capacitance of the double layer. R_{ct}: Resistance to charge transfer. Z_w: Warburg impedance.

Analytical Electrochemistry.

Supporting Electrolyte Selection. To choose the most appropriate supporting electrolyte, different electrolytes were tested (0.1 M HCl, 0.1 M H_2SO_4, 0.1 M HNO_3, 0.1 M KCl and 0.1 M acetate buffer at pH 4.6) (Figure 10). It was found that in KCl there are no appreciable peaks for either of the two species of interest, and that in HNO_3 at the selected preconcentration potential, the decomposition of the media occurs, masking the peak for Cd(II), so the use of these electrolytes was discarded. In H_2SO_4 both peaks are present, however, the current obtained for Cd(II) is low. The acetate buffer and HCl present well-defined signals for both ions, but due to the greater magnitude of the current using the second as a supporting electrolyte, it was used for the rest of the experiments.

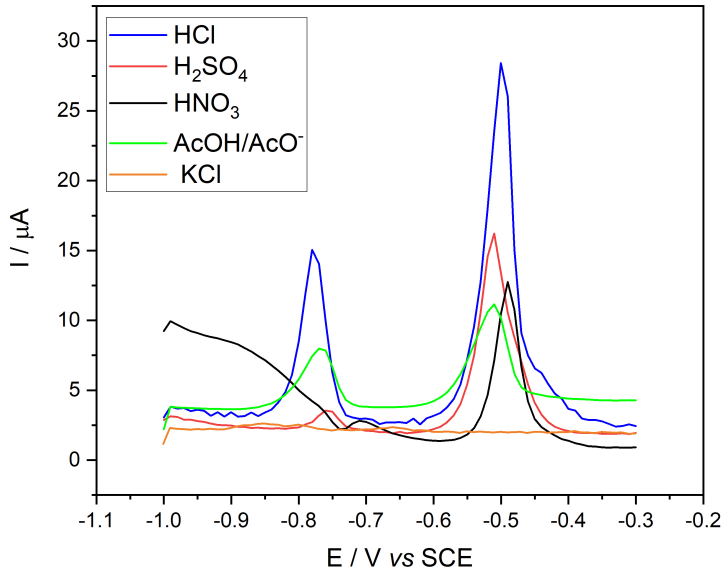

Figure 10. ASSWV (E_{dep}= -1 V, t_{dep}= 60 s, P_H= 25 mV, P_W= 50 ms, S_H= 10 mV) using a PGE in different supporting electrolytes at concentrations of Pb(II) and Cd(II) of 10 mg L^{-1}.

Preconcentration Potential and Time. The effect of the preconcentration potential on the current obtained for both analytes was evaluated (Figure 11). It was found that at potentials equal to or greater than -0.85 V *vs* SCE the obtained current for Cd(II) is null, suggesting that at these potentials the deposition of Cd on the electrode surface is not favored or that the amount deposited is too small to give a measurable signal. The highest current for both ions was recorded using -1 V as the preconcentration potential.

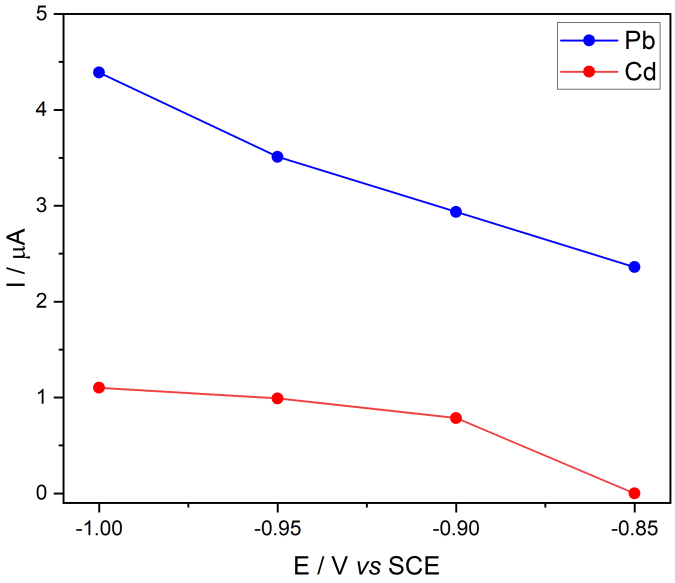

Figure 11. Optimization of the preconcentration potential for ASSWV (t_{dep}= 60 s, P_H= 25 mV, P_W= 50 ms, S_H= 10 mV) at Pb(II) and Cd(II) concentrations of 1 mg L^{-1}.

Figure 12 shows the effect of preconcentration time on the current obtained for both analytes. It was found that under the experimental conditions, a signal for Cd(II) is not registered if a preconcentration time equal to or greater than 10 s is not applied. The preconcentration time can be adjusted according to the range of concentrations to be measured. If the determinations are to be carried out at low concentrations, it is preferable to use long preconcentration times to obtain higher signals. On the contrary, at high concentrations it is convenient to use short preconcentration times to prevent electrode saturation. For the rest of the experiments, 60 s was taken as preconcentration time to optimize analysis times.

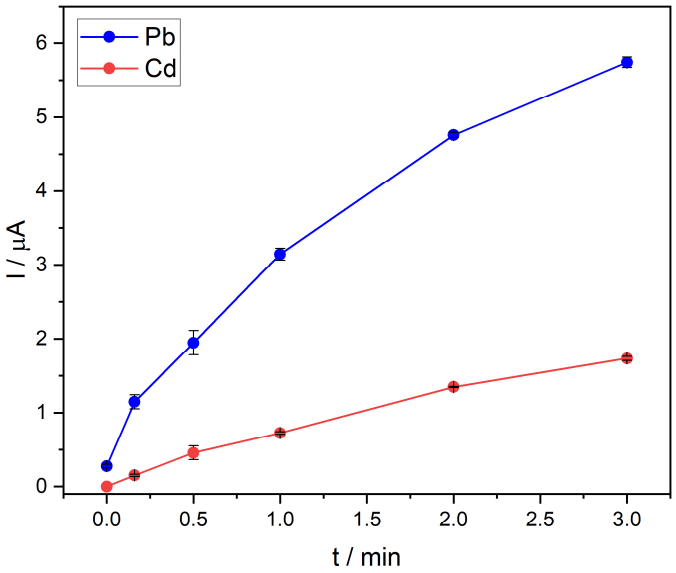

Figure 12. Optimization of preconcentration time for ASSWV (E_{dep}= -1 V, P_H= 25 mV, P_W= 50 ms, S_H= 10 mV) at Pb(II) and Cd(II) concentrations of 1 mg L^{-1}.

Anodic Stripping Step. Figure 13 shows the effect of pulse height (P_H), pulse width (P_W) and step height (S_H) on the current obtained for both metal ions. These parameters were found to be optimal values: P_H of 25 mV, P_W of 50 ms and S_H of 10 mV, because they provided lower standard deviations, greater peak to peak separation, smaller peak width, and higher currents.

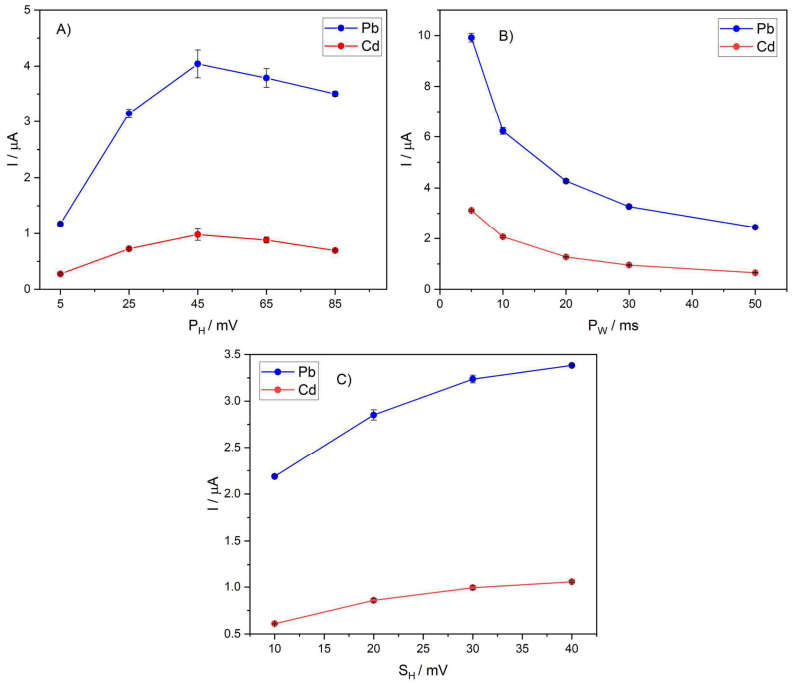

Figure 13. Optimization of P_H (A), P_W (B) and S_H (C) for ASSWV (E_{dep}= -1 V and t_{dep}= 60 s) at Pb(II) and Cd(II) concentrations of 1 mg L^{-1}.

Analytical Parameters. A simultaneous calibration curve for Pb(II) and Cd(II) between 0.8 and 100 mg L^{-1} was constructed using the optimized conditions and parameters for ASSWV (HCl 0.1 M, E_{dep}= -1 V, t_{dep}= 60 s, P_H= 25 mV, P_W= 50 ms, S_H= 10 mV) (Figure 14).

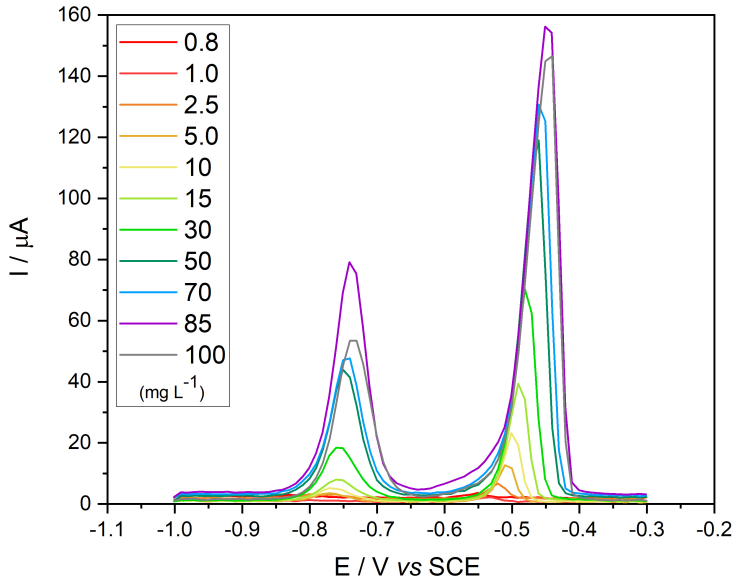

Figure 14. Optimized ASSWV (E_{dep}= -1 V, t_{dep}= 60 s, P_H= 25 mV, P_W= 50 ms, S_H= 10 mV) at Pb(II) and Cd(II) concentrations from 0.8 to 100 mg L^{-1}.

It was found that under the experimental conditions there are two linear intervals for each analyte and that, at a concentration of 100 mg L^{-1} for both ions, there is a reduction in current, which is associated to electrode saturation (Figure 15). For Cd(II) the linear intervals are from 0.8 to 10 mg L^{-1} and from 15 to 85 mg L^{-1}, while for Pb(II) it occurs from 0.8 to 30 mg L^{-1} and from 30 to 85 mg L^{-1}.

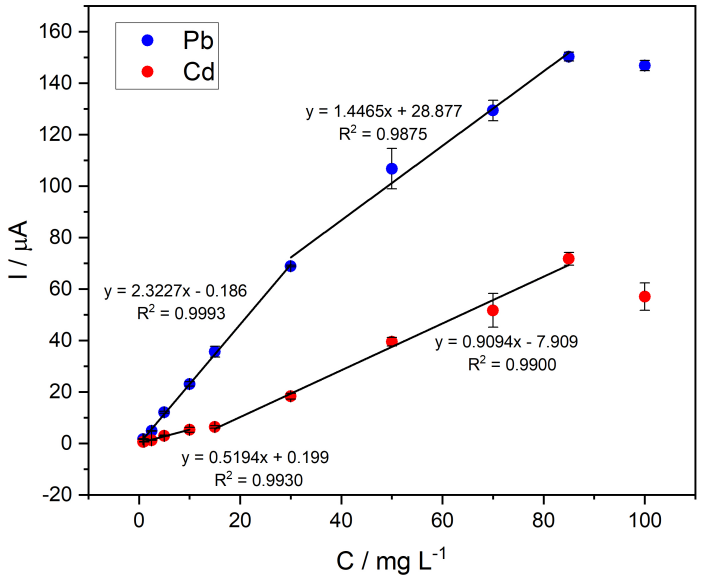

Figure 15. ASSWV calibration curve (E_{dep}= -1 V, t_{dep}= 60 s, P_H= 25 mV, P_W= 50 ms, S_H= 10 mV) using a PGE as working electrode. Cd(II) and Pb(II) 0.8, 1, 2.5, 5, 10, 15, 30, 50, 70, 85 and 100 mg L^{-1} in 0.1 M HCl.

Analytical parameters were calculated for the linear intervals (Table II), LOD and LOQ were calculated according to equations 2 and 3. Where σ is the standard deviation of the regression and m is its slope.

$$LOD = 3\sigma\ m^{-1} \quad [2]$$

$$LOQ = 10\sigma\ m^{-1} \quad [3]$$

The LOD of the lowest linear ranges were 0.946 and 1.107 mg L^{-1} for Pb(II) and Cd(II) respectively, while the LOQ of the highest concentration linear ranges were 32.934 and 33.071 mg L^{-1}.

TABLE II. Analytical parameters for the simultaneous determination of Pb(II) and Cd(II) by ASSWV with PGE as working electrode.

Analyte	Linear Range (mg L^{-1})	R^2	LOD (mg L^{-1})	LOQ (mg L^{-1})
Pb	0.8 - 30	0.9993	0.946	3.154
	30 - 85	0.9875	9.880	32.934
Cd	0.8 - 10	0.9930	1.107	3.692
	15 - 85	0.9900	9.921	33.071

Conclusions

The fabricated PGE are constituted of graphite flakes that form cavities and other structures that contribute to the rough relief of the surface of the electrode, which overall increases the electroactive area that resulted to be 2.58 times greater than its geometric area. The fabricated electrodes show a current density 0.82 times that of the GCE and reproducibility in their fabrication process and electrochemical performance.

It was found that under the experimental conditions there are two linear intervals for each analyte and it was possible to simultaneously detect Cd(II) and Pb(II) without previous modifications obtaining LOD as low as 0.946 and 1.107 mg L^{-1} for Pb(II) and Cd(II) respectively.

Due to the low cost of the proposed platform (0.20 USD per unit) it is possible to implement it in the teaching of electrochemical techniques, industrial environments or as a tool in regulatory analysis, also the proposed method can be tunned varying the preconcentration times yielding better results for different concentration ranges.

Acknowledgments

Author acknowledges Ivan Salcido from “Centro de Investigación en Ciencia y Tecnología Aplicada”, IIT-UACJ for SEM technical support.

References

1. T. Dalzochio, M. S. de Souza, L. A. R. Simões, G. J. H. Silva, G. Z. P. Rodrigues, N. B. Andriguetti, L. B. da Silva, and G. Gehlen, *Braz Arch Biol Technol.,* **62**, 1 (2019).

2. R. Das, A. T. bin Mohamed Mohtar, D. Rakshit, D. Shome, and X. Wang, *Atmos. Environt.*, **193**, 57 (2018).

3. X. Li, W. Yue, Y. Li, and G. Zhang, *J. Radioanal. Nucl. Chem.*, **266**(1), 141 (2005).

4. J. E. Forsyth, S. Nurunnahar, S. S. Islam, M. Baker, D. Yeasmin, M. S. Islam, M. Rahman, S. Fendorf, N. M. Ardoin, P. J. Winch, and S. P. Luby, *Environ. Res.*, **179**, 108722 (2019).

5. W. Kuang, Z. Chen, K. Shi, H. Sun, H. Li, L. Huang, and J. Bi, *Envoront. Int.*, **145**, (2020).

6. A. Hartwig, *Met. ions life sci.*, **11**, 491 (2013).

7. EPA, *Environmental Protection Agency,* (2022).

8. ECOL, *Diario Oficial de la Federación*, **NOM-002-ECOL-1996** (1996).

9. ECOL, *Diario Oficial de la Federación*, **NOM-001-ECOL-1996** (1996).

10. ECOL, *Diario Oficial de la Federación*, **NOM-003-ECOL-1997** (1997).

11. K. Toriumi, Y. Horikoshi, R. Yoshiyuki Osamura, Y. Yamamoto, N. Nakamura, and S. Takekoshi, *Lab. Investing.*, **93**(2), 218 (2012).

12. SCFI, *Diario Oficial de la Federación*, **NMX-AA-051-SCFI-2001** (2001).

13. J. C. Bullen, L. N. Dworsky, M. Eikelboom, M. Carriere, A. Alvarez, and P. Salaün, *PLoS One*, **17**(1), (2022).

14. S. Triantafyllidou, C. K. Nguyen, Y. Zhang, and M. A. Edwards, *Environ. Monit. Assess.*, **185**(2), 1355 (2013).

15. Annu, S. Sharma, R. Jain, and A. N. Raja, *J. Electrochem. Soc.*, 167(3), (2020).

16. S. K. Pandey, S. Sachan, and S. K. Singh, *Materials Science for Energy Technologies,* **2**(3), 667 (2019).

17. A. A. Rowe, A. J. Bonham, R. J. White, M. P. Zimmer, R. J. Yadgar, T. M. Hobza, J. W. Honea, I. Ben-Yaacov, and K. W. Plaxco, *PLoS One*, **6**(9), (2011).

18. J. R. Camargo, T. A. Silva, G. A. Rivas, and B. C. Janegitz, *Electrochim. Acta*, **409**, 139968 (2022).

19. S. Palisoc, E. M. Espique, A. M. Ribay, S. Sy, K. A. Tan, N. de Jesus, M. Noel, and M. Natividad, *Int. J. Electrochem. Sci.*, **13**(11), 10355 (2018).

20. K. C. Bedin, E. Y. Mitsuyasu, A. Ronix, A. L. Cazetta, O. Pezoti, and V. C. Almeida, *Int. J. Anal. Chem.*, **2018**, 1 (2018).

21. N. Elgrishi, K. J. Rountree, B. D. McCarthy, E. S. Rountree, T. T. Eisenhart, and J. L. Dempsey, *J. Chem. Educ.*, **95**(2), 197 (2018).

22. F. Kuralay, T. Vural, C. Bayram, E. B. Denkbas, and S. Abaci, *Colloids Surf. B*, **87**(1), 18 (2011).

23. S. Nagarajan, and R. Vairamuthu, *J. Electroanal. Chem.*, **891**, (2021).

24. A. Shah, A. Zahid, A. Khan, F. J. Iftikhar, J. Nisar, C. Fernandez, M. S. Akhter, A. A. Almutawah, and H. B. Kraatz, *J. Electrochem. Soc.*, **166**(9), B3136 (2019).

25. T. P. Lisboa, L. V. de Faria, M. A. C. Matos, R. C. Matos, R. A. de Sousa, *Microchem. J.*, **150**, 104183 (2019).

26. S. Palisoc, A. J. Gonzales, A. Pardilla, L. Racines, and M. Natividad, *Sens. Bio-Sens. Res.,* **23**, 100268 (2019).

27. P. Pinyou, V. Blay, K. Chansaenpak, and S. Lisnund, *Chemosensors*, **8**(4), 133 (2020).

28. J. Calvillo, and M. Galicia, *Int. J. Electrochem. Sci.*, **15**, 6815 (2020).

29. P. A. Flowers, and J. C. Strickland, *Spectrosc. Lett.*, **43**, 528 (2010).

30. F. E. Salih, B. Achiou, M. Ouammou, J. Bennazha, A. Ouarzane, S. A. Younssi, and M. El Rhazi, *J. Adv. Res.*, **8**(6), 669 (2017).

31. D. Eskiköy Bayraktepe, E. K. İnal, and Z. Yazan, *Microchem. J.*, **171**, 106812 (2021).